

INVESTIGATING LIPID CORONA FORMATION ONTO POLYSTYRENE
NANOPARTICLES THROUGH FLUORESCENCE CORRELATION SPECTROSCOPY

BY

LISA MANIMALETHU JACOB

THESIS

Submitted in partial fulfillment of the requirements
for the degree of Master of Science in Chemistry
in the Graduate College of the
University of Illinois Urbana-Champaign, 2015

Urbana, Illinois

Adviser:

Professor Catherine J. Murphy

ABSTRACT

When a nanoparticle enters a biological environment, molecules are known to adsorb on the surface forming a corona. Systematically studying the formation of a corona is important to develop knowledge as to how a given nanomaterial will transform once entering a biological environment. A common interface met by a nanomaterial in the human body is the cell membrane, which is composed of phospholipid bilayer. Fluorescence correlation spectroscopy (FCS) is a promising tool that can be used to probe nanoparticle-cell interactions. FCS experiments focusing on exposure of lipid vesicles to different polystyrene nanoparticles indicate possible formation of a lipid corona. Further study varying the nanoparticle charge and lipid vesicle fluidity can help elucidate the mechanism of lipid corona formation. Such work can provide insight into understanding the complex nature of the nano-bio interface.

ACKNOWLEDGEMENTS

First, I would like to thank my advisor, Professor Catherine Murphy for her help, support, and guidance. I would like to thank all of the members of the Murphy research group and the Center for Sustainable Nanotechnology who have helped me through insightful discussions, instructions and collaborations.

I would like to thank Dr. Dianwen Zhang of the Beckman Institute, Dr. John King of the Granick group, and Michael Hallock at UIUC for useful discussions and advice in regards to this work.

I would like to thank friends and mentors both new and old for their words of wisdom and support. Lastly, thank you to my family for their ceaseless love and support. I would not have been able to complete this thesis without their patience and prayers.

TABLE OF CONTENTS

Chapter 1: INTRODUCTION TO NANOPARTICLE-BIOMOLECULE INTERACTIONS..	1
1.1 Introduction	1
1.2 References.....	10
Chapter 2: INVESTIGATING LIPID CORONA FORMATION ONTO POLYSTYRENE NANOPARTICLE THROUGH FLUORESCENCE CORRELATION SPECTROSCOPY	13
2.1 Materials	13
2.2 Instrumentation	13
2.3 References.....	26
Chapter 3: CONCLUSIONS AND FUTURE WORK	27

Chapter 1: INTRODUCTION TO NANOPARTICLE-BIOMOLECULE INTERACTIONS

1.1 Introduction

The unintended impact of nanomaterials when exposed to biological systems is a question of increasing importance, as various nanomaterial constructs are employed in the fields of medicine and biotechnology for varying applications as depicted in Figure 1.1.¹ During exposure, biological molecules, such as proteins², sugars³, and lipids⁴ may adsorb to the nanomaterial. This phenomenon can then alter the function and fate of the nanomaterial because what is recognized by biological systems, such as cells, is the nanomaterial-biomolecule complex.⁵ Given that the function of and biological response to nanomaterials depends largely on the nanomaterial surface², it is critical to systematically study the nano-bio interface.

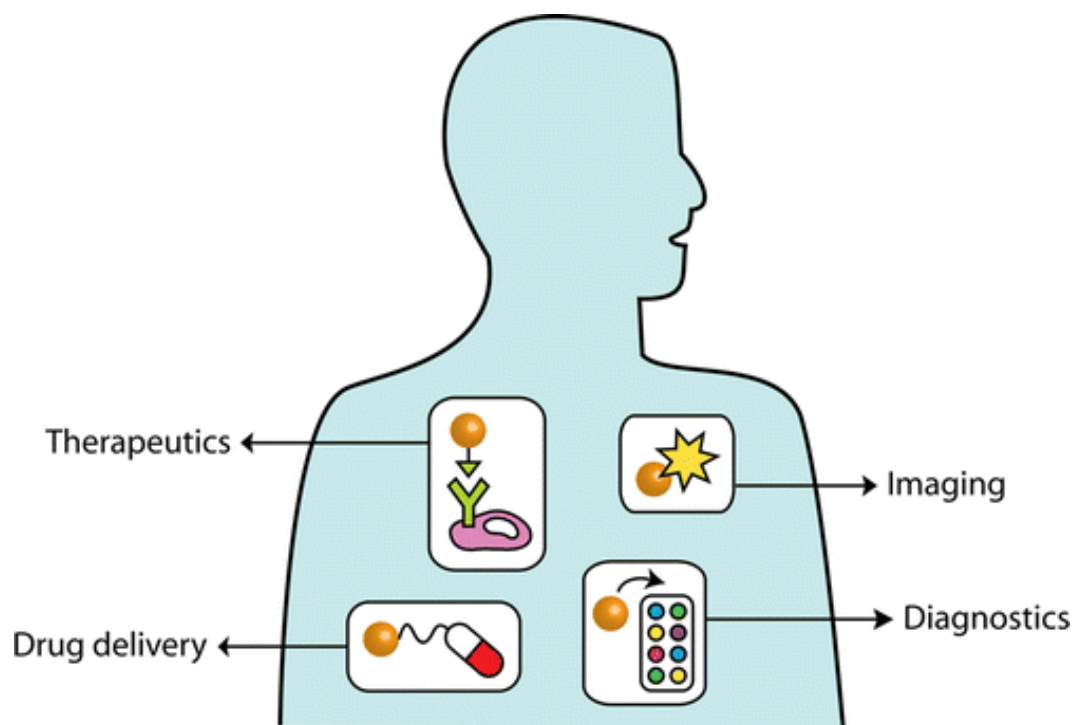


Figure 1.1. Understanding the implications of biomolecule adsorption onto nanoparticle surfaces is important for various medical applications in which nanomaterials are employed.¹

Of the various nanomaterial-biomolecule interactions investigated, nanoparticle-protein interactions are the most well-studied. Previously, researchers have found that proteins adsorb onto the surface of nanomaterials, forming a protein corona.^{2,5} The nanoparticle-protein complex is a dynamic system; proteins can adsorb and desorb onto the nanoparticle surface or off of already-bound proteins.⁶ Knowledge of the dynamics of adsorption such as binding affinities and rates of adsorption and desorption is one critical component to understanding nano-bio interactions because this partly dictates how biological systems recognize and respond to the nanomaterial.

Although a great deal of research has focused on extensively studying the protein corona, adsorption of other biomolecules, such as lipids, to nanoparticle surfaces is less studied and warrants scientific research. Biological systems, such as cells, are complex. When a nanomaterial comes into contact with a cell, the surfaces that meet are the nanoparticle surface and the cell membrane. The cell membrane consists primarily of a phospholipid bilayer. Previous work focused on understanding nanoparticle-cell interactions has largely considered effects of nanomaterial exposure to model cell membrane systems. For example, Holl and coworkers have conducted a number of studies investigating the effects of cationic nanoparticles when exposed to supported lipid bilayer systems.^{7,8} Specifically, dimyristoylphosphatidylcholine (DMPC), was the primary lipid used to form the supported bilayers. These studies demonstrated that both organic (dendrimer) and inorganic (gold and silica) nanoparticles functionalized with positively-charged surfaces resulted in membrane thinning or disruption after exposure. This work provides important context for the described work herein but primarily takes the perspective of what occurs to the experimental model of

the cell, rather than the nanomaterial. Further scientific exploration must be devoted to understanding nanoparticle-cell interactions, specifically in the point of view of the nanomaterial. This undertaking is necessary as nanomaterials are being employed for medical applications.

Understanding nano-bio interactions is challenging because probing what happens at this interface requires many complementary techniques to yield a full and accurate description.⁹ Researchers have employed a variety of analytical techniques to understand nanomaterial-biomolecule interactions, such as, UV-vis spectroscopy, FT-IR, ζ -potential analysis, dynamic light scattering, isothermal titration calorimetry, quartz crystal microbalance, and 2D-NMR.^{10,11,12,13,14} The number of techniques used to study the protein corona highlights the experimental difficulty in understanding nano-bio interactions in general. Fluorescence correlation spectroscopy (FCS) is a potential technique that can provide dynamic and kinetic information on lipid adsorption chemistry to nanoparticle surfaces. FCS is a fluorescence fluctuation correlation spectroscopy and can be considered the fluorescent analog of dynamic light scattering.¹⁵ In other words, FCS is most commonly used to obtain the hydrodynamic diameter of a fluorescent species *in situ* by from its diffusion behavior. A representative diagram of the typical FCS instrument is shown in Figure 1.2. FCS is an advantageous technique because the experiment is done *in situ* and therefore no washing or centrifugation is necessary, allowing FCS to be used to track the diffusion of a fluorescent probe within a cell and living organisms.¹⁵ This latter advantage of FCS is compelling; the possibility of tracking a nanoparticle within a cell, as it interacts with its local environment is not a possibility with the techniques previously aforementioned. The ultimate experiment in

understanding nano-bio interactions is tracking the nanomaterial inside a cell or living organism and obtaining real-time chemical information.

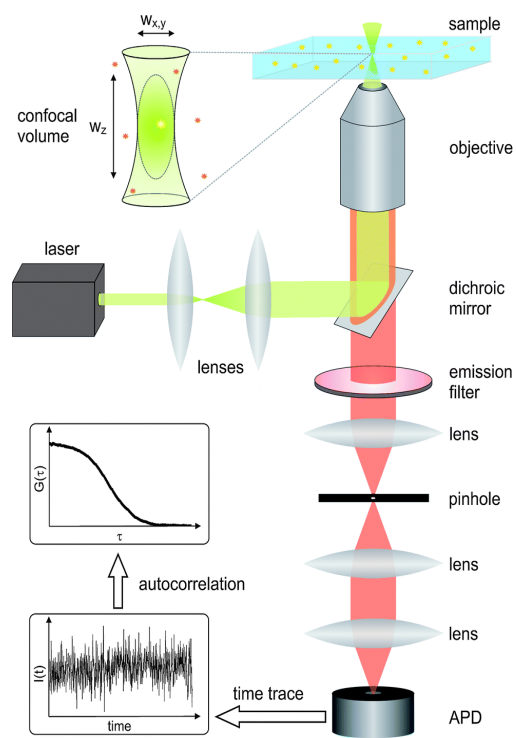


Figure 1.2. A diagram of a standard FCS instrument. ¹⁶

The main focus of the work described herein is using FCS to understand the interactions of nanoparticles with lipid vesicles to provide insight into nanoparticle-cell interactions. Specifically, we aim to obtain dynamic information about nanoparticles as they interact with an experimental model of a cell membrane. We have explored this question by using suspended lipid vesicles as a simple model of the cell membrane. As schematically depicted in Figure 1.3, the main research question is first; does a lipid corona form around fluorescent nanoparticles? Secondly, can we use FCS to obtain dynamic information, such as association/dissociation rates and binding constants?

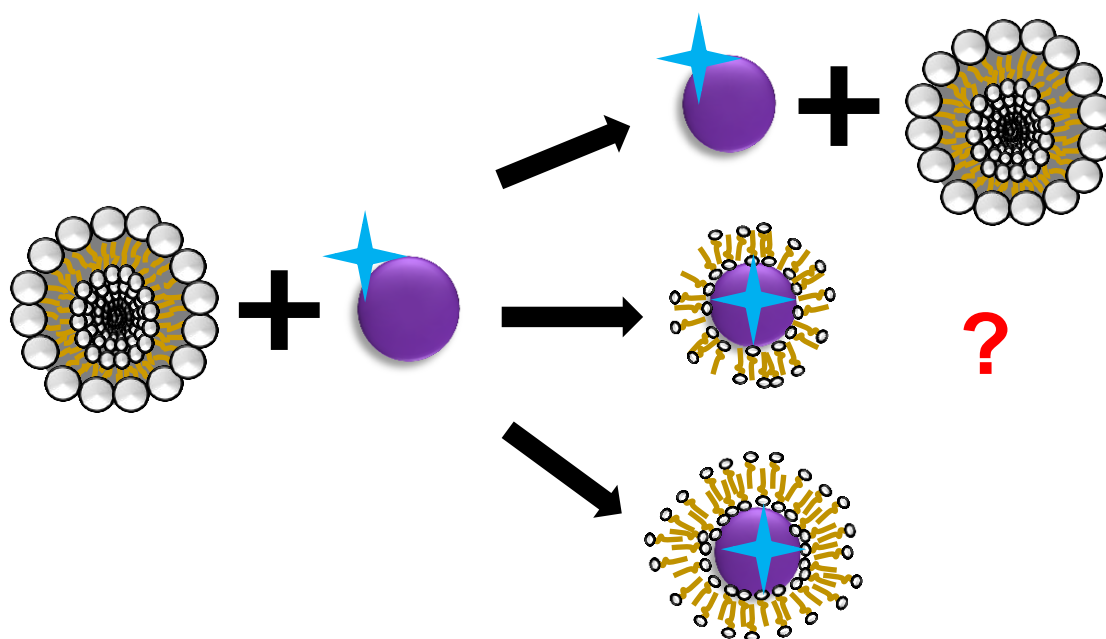


Figure 1.3. Schematic diagram of main experiment, exposure of lipid vesicles to fluorescent nanoparticles.

We decided to investigate the effect of nanoparticle surface chemistry to understand how the role of electrostatics will affect possible lipid corona formation. Two types of intrinsically fluorescent polystyrene nanoparticles modified with amine groups, PS/NH₂ and carboxyl groups, PS/COOH NPs, obtained from a commercial source were used to initially test and understand lipid corona formation through FCS. Nitrogen-vacancy center nanodiamond, Nv ND, an intrinsically fluorescent nanomaterial, was also explored. However, several experimental difficulties prohibited its use for experiments. A brief summary of the problems associated with Nv ND will follow in the next chapter.

Both types of fluorescent polystyrene nanoparticles are from a commercial source (Bangs Laboratories) and are reported to be ~60 nm in diameter. They are encapsulated with a green-emitting fluorophore called “dragon green”, with appreciable excitation at 470 nm, although its chemical identity is proprietary information. The precise surface chemistry of the two types of polystyrene nanoparticles is unknown because the identity of the surface ligands is proprietary information.

Nitrogen-vacancy center nanodiamond, an all-carbon material in the nanoscale size regime, has garnered considerable research interest recently. Nv ND has favorable mechanical properties, good chemical stability and easy surface functionalization.¹⁷ Nv ND consists of a network of sp³ carbon atoms and the surface is terminated with sp² carbons. Nv ND has strong fluorescence and biocompatibility, making it useful for biomedical applications. The fluorescence of Nv ND arises from the formation of nitrogen-vacancy centers in the crystal structure. As synthesized, ND naturally possesses nitrogen atoms. Irradiation of ND with high energy particles forms

vacancies.¹⁸ The vacancies migrate and get trapped by nitrogen atoms upon annealing. Two types of defect centers form, a neutral vacancy and negatively-charged vacancy, producing two different fluorescent emissions. The negatively charged vacancy, Nv^- , is of greater use because it has a spin state of 1 and a long spin coherence time compared to the other vacancy. A schematic representation of Nv^- defect is shown in Figure 1.4.¹⁷ This vacancy is known to have an excitation maximum of 565 nm and emission maximum of 685 nm and molar extinction coefficient of $8000 \text{ M}^{-1}\text{cm}^{-1}$.¹⁹ This molar extinction coefficient is 1-2 orders of magnitude lower than a standard fluorophore. Therefore, Nv^- ND has weaker intrinsic fluorescence compared to a typical fluorophore. Given its favorable properties and intrinsic fluorescence, Nv^- ND is gaining interest as a favorable candidate for use in medical applications.

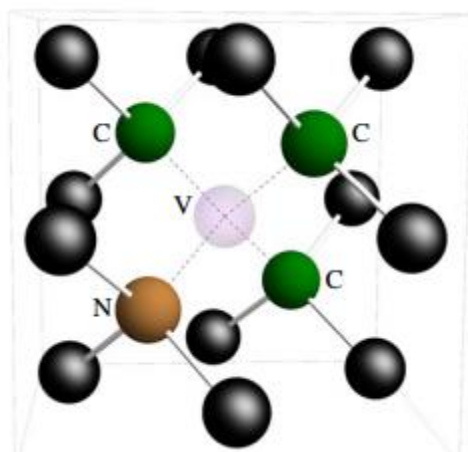


Figure 1.4. Schematic of chemical structure of a nitrogen-vacancy center in Nv^- ND. Figure adapted from reference 20.²⁰

Lipids were chosen to represent a model cell membrane. The phosphatidylcholine (PC) head group, indicated by the green circle in Figure 1.5., is of important biological relevance because it is one of the major constituents in eukaryotic cell membranes.²¹ Two lipids were chosen for initial studies, 2-dimyristoyl-*sn*-glycero-3-phosphocholine (DMPC) and 1,2-ditetradecanoyl-*sn*-glycero-3-phospho-(1'-*rac*-glycerol) (DMPG), as shown in Figure 1.5. An important property of lipids is the phase transition temperature, which is the temperature required to induce a change from the ordered gel state to the disordered liquid crystalline phase. The transition temperatures of both DMPC and DMPG is 23°C, therefore resulting lipid vesicles will be at the gel/liquid crystalline transition at room temperature.²²

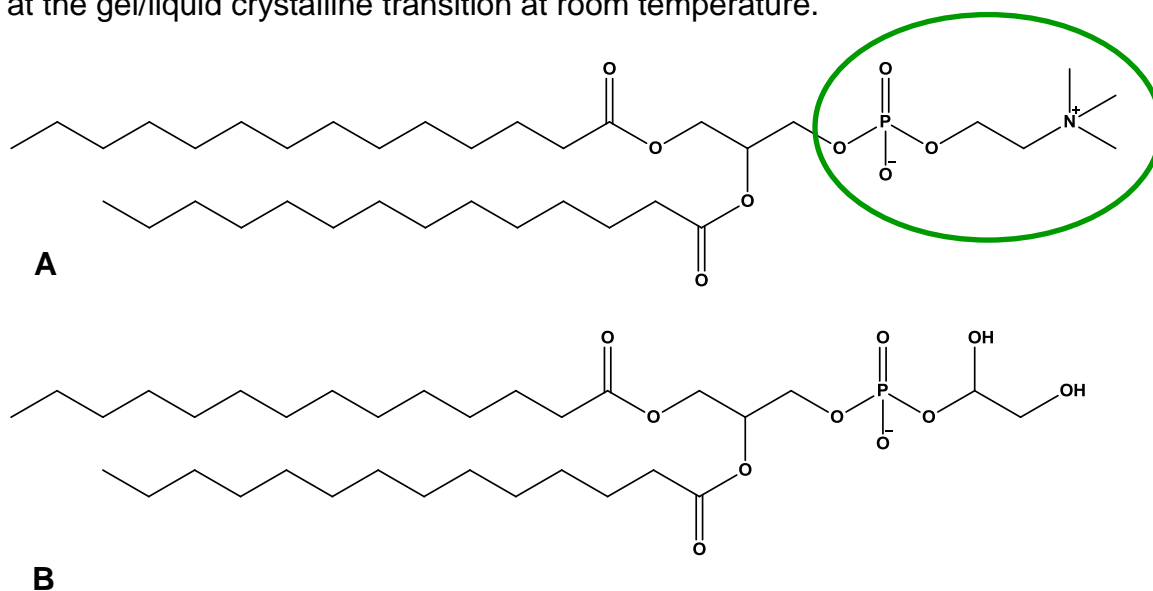


Figure 1.5. Chemical structures of A) DMPC with PC group encircled in green and B) DMPG.

1.2 References

1. Murphy, C. J.; Vartanian, A. M.; Geiger, F. M.; Hamers, R. J.; Pedersen, J.; Cui, Q.; Haynes, C. L.; Carlson, E. E.; Hernandez, R.; Klaper, R. D.; Orr, G.; Rosenzweig, Z. e., Biological Responses to Engineered Nanomaterials: Needs for the Next Decade. *ACS Central Science* **2015**, 1 (3), 117-123.
2. Cedervall, T.; Lynch, I.; Lindman, S.; Berggård, T.; Thulin, E.; Nilsson, H.; Dawson, K. A.; Linse, S., Understanding the nanoparticle–protein corona using methods to quantify exchange rates and affinities of proteins for nanoparticles. *Proceedings of the National Academy of Sciences* **2007**, 104 (7), 2050-2055.
3. Hellstrand, E.; Lynch, I.; Andersson, A.; Drakenberg, T.; Dahlbäck, B.; Dawson, K. A.; Linse, S.; Cedervall, T., Complete high-density lipoproteins in nanoparticle corona. *FEBS Journal* **2009**, 276 (12), 3372-3381.
4. Wan, S.; Kelly, P. M.; Mahon, E.; Stöckmann, H.; Rudd, P. M.; Caruso, F.; Dawson, K. A.; Yan, Y.; Monopoli, M. P., The “Sweet” Side of the Protein Corona: Effects of Glycosylation on Nanoparticle–Cell Interactions. *ACS Nano* **2015**, 9 (2), 2157-2166.
5. Lynch, I.; Cedervall, T.; Lundqvist, M.; Cabaleiro-Lago, C.; Linse, S.; Dawson, K. A., The nanoparticle–protein complex as a biological entity; a complex fluids and surface science challenge for the 21st century. *Advances in Colloid and Interface Science* **2007**, 134, 167-174.
6. Casals, E.; Pfaller, T.; Duschl, A.; Oostingh, G. J.; Puentes, V., Time Evolution of the Nanoparticle Protein Corona. *ACS Nano* **2010**, 4 (7), 3623-3632.
7. Leroueil, P. R.; Hong, S.; Mecke, A.; Baker, J. R.; Orr, B. G.; Banaszak Holl, M. M., Nanoparticle Interaction with Biological Membranes: Does Nanotechnology Present a Janus Face? *Accounts of Chemical Research* **2007**, 40 (5), 335-342.
8. Leroueil, P. R.; Berry, S. A.; Duthie, K.; Han, G.; Rotello, V. M.; McNerny, D. Q.; Baker, J. R.; Orr, B. G.; Banaszak Holl, M. M., Wide Varieties of Cationic Nanoparticles Induce Defects in Supported Lipid Bilayers. *Nano Letters* **2008**, 8 (2), 420-424.
9. Nel, A. E.; Madler, L.; Velegol, D.; Xia, T.; Hoek, E. M. V.; Somasundaran, P.; Klaessig, F.; Castranova, V.; Thompson, M., Understanding biophysicochemical interactions at the nano-bio interface. *Nat Mater* **2009**, 8 (7), 543-557.
10. Aubin-Tam, M.-E.; Hamad-Schifferli, K., Gold Nanoparticle–Cytochrome c Complexes: The Effect of Nanoparticle Ligand Charge on Protein Structure. *Langmuir* **2005**, 21 (26), 12080-12084.

11. Deka, J.; Paul, A.; Chattopadhyay, A., Estimating conformation content of a protein using citrate-stabilized Au nanoparticles. *Nanoscale* **2010**, 2 (8), 1405-1412.
12. Lundqvist, M.; Nygren, P.; Jonsson, B.-H.; Broo, K., Induction of Structure and Function in a Designed Peptide upon Adsorption on a Silica Nanoparticle. *Angewandte Chemie* **2006**, 118 (48), 8349-8353.
13. Brewer, S. H.; Glomm, W. R.; Johnson, M. C.; Knag, M. K.; Franzen, S., Probing BSA Binding to Citrate-Coated Gold Nanoparticles and Surfaces. *Langmuir* **2005**, 21 (20), 9303-9307.
14. Troiano, J. M.; Olenick, L. L.; Kuech, T. R.; Melby, E. S.; Hu, D.; Lohse, S. E.; Mensch, A. C.; Dogangun, M.; Vartanian, A. M.; Torelli, M. D.; Ehimighe, E.; Walter, S. R.; Fu, L.; Anderton, C. R.; Zhu, Z.; Wang, H.; Orr, G.; Murphy, C. J.; Hamers, R. J.; Pedersen, J. A.; Geiger, F. M., Direct Probes of 4 nm Diameter Gold Nanoparticles Interacting with Supported Lipid Bilayers. *The Journal of Physical Chemistry C* **2015**, 119 (1), 534-546.
15. Ries, J.; Schwille, P., Fluorescence correlation spectroscopy. *BioEssays* **2012**, 34 (5), 361-368.
16. Ehrenberg, M.; Rigler, R., Rotational brownian motion and fluorescence intensify fluctuations. *Chemical Physics* **1974**, 4 (3), 390-401.
17. Mochalin, V. N.; Shenderova, O.; Ho, D.; Gogotsi, Y., The properties and applications of nanodiamonds. *Nat. Nanotechnol.* **2012**, 7 (Copyright (C) 2014 American Chemical Society (ACS). All Rights Reserved.), 11-23.
18. Slepetz, B.; Laszlo, I.; Gogotsi, Y.; Hyde-Volpe, D.; Kertesz, M., Characterization of large vacancy clusters in diamond from a generational algorithm using tight binding density functional theory. *Physical Chemistry Chemical Physics* **2010**, 12 (42), 14017-14022.
19. Mohan, N.; Tzeng, Y.-K.; Yang, L.; Chen, Y.-Y.; Hui, Y. Y.; Fang, C.-Y.; Chang, H.-C., Sub-20-nm Fluorescent Nanodiamonds as Photostable Biolabels and Fluorescence Resonance Energy Transfer Donors. *Advanced Materials* **2010**, 22 (7), 843-847.
20. Schirhagl, R.; Chang, K.; Loretz, M.; Degen, C. L., Nitrogen-Vacancy Centers in Diamond: Nanoscale Sensors for Physics and Biology. *Annual Review of Physical Chemistry* **2014**, 65 (1), 83-105.
21. Yeagle, P. L., *The Membranes of Cells*. Academic Press: Boston, 1993.

22. Szoka, F.; Papahadjopoulos, D., Comparative Properties and Methods of Preparation of Lipid Vesicles (Liposomes). *Annual Review of Biophysics and Bioengineering* **1980**, 9 (1), 467-508.

Chapter 2: INVESTIGATING LIPID CORONA FORMATION ONTO POLYSTYRENE NANOPARTICLE THROUGH FLUORESCENCE CORRELATION SPECTROSCOPY

2.1 Materials

Two different surface-modified polystyrene nanoparticles encapsulated with fluorophore, PS/NH₂ and PS/COOH, were purchased commercially from Bangs Lab and used following initial testing using a fluorimeter to confirm fluorescence. Bovine serum albumin (BSA) was purchased from Sigma Life Sciences. All lipids were obtained from Avanti Polar Lipids and arrived dissolved in chloroform. Nitrogen-vacancy center nanodiamond was obtained from Microdiamant© and Adamas© and either used directly or surface-modified by polyelectrolyte wrapping by the Hamers group, CSN collaborator. Tris base, from Fisher Bioreagents, was used for all experiments discussed. GR ACS sodium chloride was purchased from EMD Millipore. Purified 18 MΩ water was used for all experiments..

2.2 Instrumentation

Fluorescence measurements were performed on a Jobin Yvon Fluoromax-3 spectrophotometer. Transmission electron microscopy (TEM) was performed using a Hitachi H600 Transmission Electron Microscope at 75 KV. Zeta potential measurements were obtained using a Brookhaven ZetaPALS instrument. Single-photon FCS measurements were conducted using the ISS Alba FCS instrument with a 470 nm diode laser for excitation possessing 3 mW power and a 60x lens with 1.2 numerical aperture.

Lipid Vesicle Preparation

Small unilamellar lipid vesicles were prepared by extrusion through a 0.05 μm membrane filter using a lipid extruder kit. The lipid vesicles were prepared in a buffer solution of 10 mM tris, 100 mM NaCl, and pH 7.4 and this buffer was used for all discussed experiments. The fluorescent polystyrene nanoparticles were characterized first by a fluorimeter to confirm its fluorescence, dynamic light scattering for hydrodynamic size, and zeta-potential measurements for surface charge.

General Experimental Methods for FCS Studies

For the equilibrium interaction studies, both nanoparticle and lipid vesicle analytes were added to Eppendorf tubes and allowed to interact overnight for a period of at least 24 hours for equilibration. 400 μL aliquots of each sample were then transferred to an 8-well, polystyrene chambered 1.0 (170 μm) borosilicate coverglass culture plate (Lab-Tek, Thermo Scientific Nunc®). The well plates are sterile and are used only once before disposal. Prior to taking aliquots of the samples, the well-plates were pre-coated with a 1% (10 mg/mL) BSA blocking solution to prevent adsorption onto well surfaces, rinsed with buffer, and air-dried.

For each sample, at least five to seven replicate measurements were taken. It is important to take multiple measurements of each sample because the fluorescence signal is extremely sensitive and the occurrence of sporadic agglomeration will generate a high fluorescence signal that will overwhelm the actual signal of individual fluorescent analytes moving through the confocal detection volume. The dimensions of the FCS confocal detection volume must be determined before every FCS experiment. This step

is important to obtain accurate diffusion times of the analyte. To do this, a well-studied and strongly fluorescent dye is used and autocorrelation curves are calculated. Rhodamine 110 dye in water is used at a concentration of 1 nM and five replicate measurements are typically taken. The laser intensity was 65%, leading to ~30,000 counts per second. The raw data was processed for autocorrelation analysis and τ_D values were fit. Rhodamine 110 has a diffusion coefficient of $3.979 \times 10^{-10} \text{ m}^2/\text{sec}$ at 19°C as determined from a temperature-corrected equation.¹ The delay time values determined from autocorrelation analysis of the standard were used to obtain the radius of the confocal volume values for each run by setting the diffusion coefficient to the standard value of $3.979 \times 10^{-10} \text{ m}^2/\text{sec}$.

Diffusion Equation and FCS Raw Data Processing

After obtaining the raw fluorescence fluctuation data, it must be further processed through autocorrelation analysis to obtain information such as diffusion coefficients, diffusion times, concentrations, and hydrodynamic size for spherical analytes, using the Stokes-Einstein equation. The autocorrelation function is defined to be:

Equation 2.1
$$G(\tau) = \frac{\langle \delta F(t) \delta F(t+\tau) \rangle}{\langle F(t) \rangle^2}$$

where $\delta F(t) = F(t) - \langle F(t) \rangle$

and $\delta F(t + \tau) = F(t + \tau) - \langle F(t + \tau) \rangle$

F is defined as the fluorescence intensity at time t , and τ , is the time delay.

The autocorrelation function can be described by a 3D Gaussian distribution for objects randomly diffusing in 3 dimensions in a confocal volume. This transforms $G(\tau)$ to:

Equation 2.2

$$G(\tau) = \frac{1}{N} \left(\frac{1}{1 + \frac{\tau}{\tau_D}} \right) \left(\frac{1}{1 + \frac{\tau}{\tau_D} \left(\frac{\omega_0}{\omega_z} \right)^2} \right)^{1/2}$$

where N is the number of detected objects and is related to concentration, C, and volume, V, by the equation $N=VC$, τ_d is the diffusion time or time delay of an object within the confocal volume and ω_o/ω_z is the structure parameter, where ω_o , is the confocal volume radius, and ω_z is the height of the confocal volume. The confocal volume can be thought to have a shape as shown in Figure 2.1

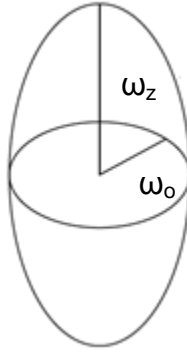


Figure 2.1. Approximate shape of the FCS detection volume. Figure adapted from reference 15.

The autocorrelation function can be further transformed to the following equation which is used to apply the curve fits to the plotted autocorrelation curve in the FCS studies described later.

Equation 2.3

$$G(\tau) = G_o \left(\frac{1}{1 + \frac{\tau}{\tau_D}} \right) \left(\frac{1}{1 + \frac{\tau}{\tau_D} (\alpha^{-2})} \right)^{1/2} + G_\infty$$

G_o is equal to $\frac{1}{N}$ and α is the structure parameter described previously and is equal to ω_z/ω_o , G_∞ is the autocorrelation function at infinite τ which should theoretically be zero. In processing FCS data, the four parameters, τ_D , α , G_o , and G_∞ are manually inserted into the IgorPro fitting program and the program takes the four initial values as guesses and manipulates the curve to minimize the chi-squared fitting parameter. From the fit to the autocorrelation plot, the most important value that can be determined is τ_D , which gives us information on the diffusion coefficient, D , and hydrodynamic diameter, D_H , of spherical analytes.

The diffusion time or time delay and the diffusion coefficient are related by the following equation:

Equation 2.4
$$\tau_D = \frac{\omega_o^2}{4D}$$

so it is necessary to determine the radius of the confocal detection volume of the FCS instrument through a standard fluorescing dye.

The Stokes-Einstein equation is applicable to spherical analytes and relates the diffusion coefficient to the hydrodynamic size (shown below as hydrodynamic diameter):

Equation 2.5
$$D = \frac{k_B T}{3\pi\eta D_H}$$

A simple way to check the accuracy of FCS measurements is to compare the hydrodynamic size of the spherical particle measured through FCS to its value as measured by dynamic light scattering, which will be discussed later.

FCS Data Processing

The fluorescence fluctuation or “raw” data for all measurements were saved and subject to autocorrelation analysis. Autocorrelation analysis is performed for each measurement individually. The raw data contains the time and measured counts per unit time. Autocorrelation analysis was done using a program written in collaboration with Professor Robert Hamers (UW-Madison) and modified by Michael Hallock (UIUC) which calculates the autocorrelation function $G(\tau)$ at various tau values. This step is done through the UIUC computing cluster and generates the τ and $G(\tau)$ values. These values are plotted in an advanced graphing software, IGOR Pro, and the autocorrelation curve fit is applied to each plot, as described in the previous sections above. All replicate measurements were then subject to the q-test at 90% confidence intervals and those remaining were considered for calculations.

These experiments aim to investigate the dynamic events that occur when nanoparticles are exposed to lipid vesicles and determine if a lipid corona is formed around the nanoparticles. Fluorescent polystyrene nanoparticles of varying surface chemistry were used to understand the mechanism of lipid corona formation.

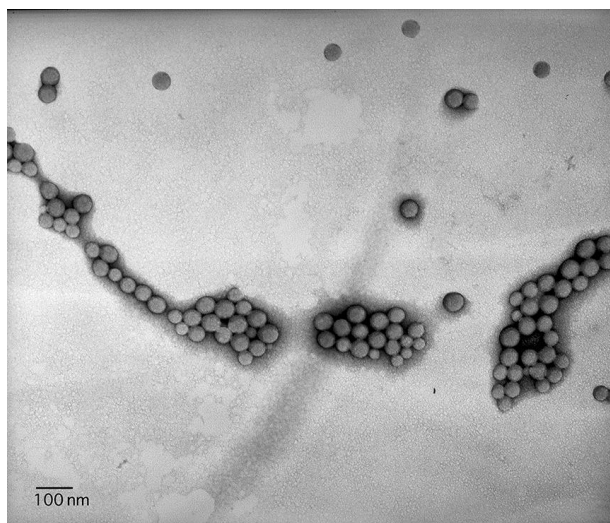
Interaction studies of Fluorescent Polystyrene Nanoparticles with Lipid Vesicles

Considering the work done by Holl and coworkers previously discussed and emerging work within the CSN examining the effect of mostly DMPC and DOPC supported lipid bilayers with cationic nanoparticles² we expected PS/NH₂ and suspended lipid vesicles to interact and form a lipid corona through electrostatic interactions. If lipid corona formation were strongly electrostatically dependent,

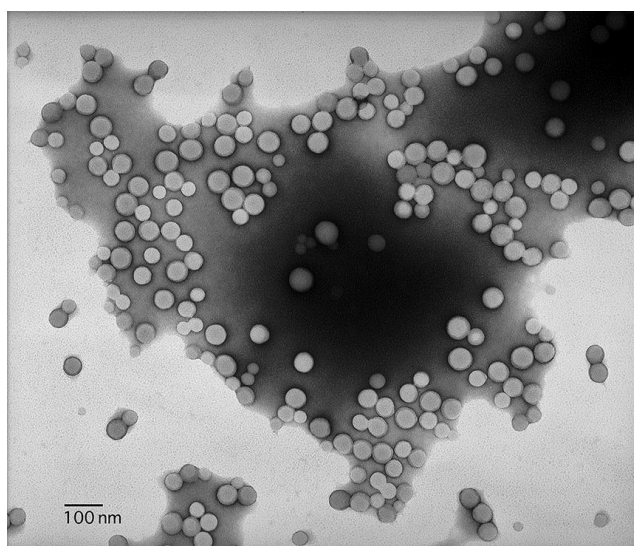
incubation of lipid vesicle with PS/COOH would result in formation in lipid corona and therefore no change in hydrodynamic diameter. Both types of nanoparticles and lipid vesicle were characterized via DLS and zeta-potential measurements, shown in Table 2.1. The hydrodynamic diameters of the nominal 60 nm polystyrene nanoparticles were found to be around 60 nm in diameter and yielded expected surface charges given the surface chemistry. The hydrodynamic diameter and surface charge of the lipid vesicle was as expected, given that DMPG is a negatively charged lipid so addition of DMPG would yield negatively-charged lipid vesicles. Transmission electron micrographs of both polystyrene nanoparticles revealed fairly uniform, spherical nanoparticles of approximately 60 nm in diameter, as shown in Figure 2.2.

Table 2.1. Dynamic light scattering and zeta-potential data of polystyrene nanoparticles and lipid vesicles prior to interaction study in buffer conditions, 10 mM tris, 100 mM NaCl, pH 7.4.

System	D_H (nm)	ζ-Potential (mV)
60 nm PS/NH ₂	57.1 ± 0.2	+31.00 ± 1.47
60 nm PS/COOH	75.0 ± 0.3	-19.93 ± 1.40
9:1 DMPC:DMPG	124.7 ± 0.9	-20.68 ± 1.07



A



B

Figure 2.2. Transmission electron microscopy images of A) amine B) carboxyl-terminated polystyrene nanoparticles stained with 2% ammonium molybdate. Images were taken by Lou Ann Miller.

FCS experiments of PS/NH₂ and PS/COOH incubated with 9:1 DMPC:DMPG lipid vesicles yielded interesting results, the trend in hydrodynamic sizes as presented in Figure 2.3 A), indicate that possible lipid corona formation is occurring in the presence of PS/NH₂ nanoparticles, while the results are mixed for PS/COOH NPs, as shown in Figure 2.3 B).

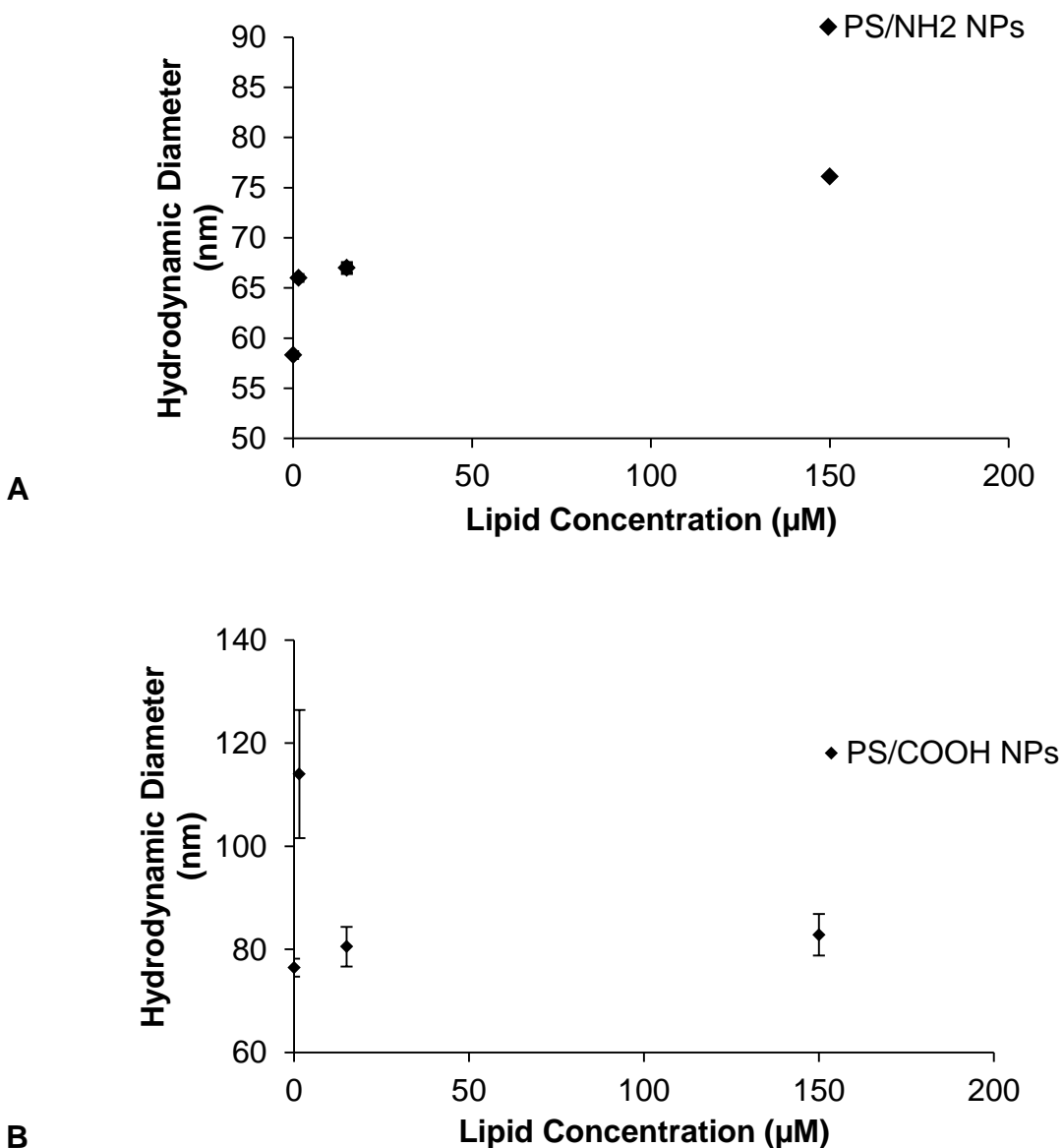


Figure 2.3. Lipid adsorption isotherm plots of A) 1 nM carboxyl B) 1 nM amine-terminated polystyrene nanoparticles after addition of 9:1 DMPC:DMPG lipid vesicles in 10 nM tris buffer, 100 nM NaCl, pH 7.4.

Given Table 2.2, addition of lipid vesicle resulted in increases in hydrodynamic diameter however the trend was different depending on particle type. Addition of lipid vesicle to PS/COOH NPs resulted in increases in hydrodynamic diameter but there was no gradual trend. Rather the change was abrupt, with an increase of 37.5 ± 14.1 nm upon initial addition of lipid, however further additions of lipid resulted in a smaller change of hydrodynamic diameter from bare nanoparticle. For PS/NH₂ NPs, each addition of lipid vesicle resulted in gradual increase in hydrodynamic diameter, indicating the possibility of lipid corona formation. Given that the lipid vesicles are primarily composed of DMPC, the length of a fully extended DMPC molecule is approximately 3.9 nm, assuming carbon-carbon single bonds. The changes in hydrodynamic diameter of $7.2 \text{ nm} \pm 0.4 \text{ nm}$ and $8.7 \text{ nm} \pm 0.4 \text{ nm}$ can suggest the formation of a bilayer. An increase of $17.3 \text{ nm} \pm 0.7 \text{ nm}$ suggests the formation of two bilayers. These studies need to be repeated for further confirmation of lipid corona formation.

Table 2.2. Measured hydrodynamic diameter and change in hydrodynamic diameter of polystyrene nanoparticles upon addition of 9:1 DMPC:DMPG lipid vesicle.

Sample	D _H (nm)	Δ D _H (nm)
1 nM PS/COOH	76.5 ± 1.7	---
+1.5 μM	114.0 ± 12.4	37.5 ± 14.1
+15 μM	80.5 ± 3.8	4.0 ± 5.5
+150 μM	82.8 ± 4.0	6.3 ± 5.7
1 nM PS/NH ₂	58.3 ± 0.2	---
+1.5 μM	66.0 ± 0.2	$+7.2 \pm 0.4$
+15 μM	67.0 ± 0.2	$+8.7 \pm 0.4$
+150 μM	76.1 ± 0.5	$+17.3 \pm 0.7$

Future experiments would entail repeating experiments and including a neutral surface to understand the role of electrostatics in lipid corona formation. The mammalian cell membrane is known to have more and less fluid areas given different components in the cell membrane can have a stiffening effect, such as the presence of cholesterol, a hydrophobic molecule.³ Therefore, lipids of different transition temperatures can be used to vary the lipid vesicle fluidity. It is difficult to determine how the lipids adsorb and precise packing information. Lipids are known to form bilayers, in particular if the lipids contain two chains and the size of the nanoparticle is greater than 22 nm.⁴ Future work would entail cryo-TEM experiments of the polystyrene nanoparticles following incubation to hopefully reveal lipids on the surface. It is important to note that DLS experiments measuring the hydrodynamic size of only the polystyrene nanoparticles are difficult because the scattering signal output is a combination from both lipid vesicles and nanoparticles that are similar in size, resulting in unreliable data that is difficult to deconvolute.

Nv ND

Two types of Nv ND were available for studies; 1) 25 nm and 2) 100 nm. As shown in Figure 2.4.A), the UV-vis absorbance spectra displayed slight absorbance at the laser wavelength available (470 nm). Furthermore, from Figure 2.4, the 25 nm NV ND yielded poor fluorescence, while the 100 nm size core, while demonstrating appreciable fluorescence, had poor colloidal stability. Confocal Raman data (spectra not shown) reveal a large Raman scattering signal from water, given that all experiments are done in water, which overwhelms the weak fluorescence signal. A poor

fluorescence signal is difficult to overcome for FCS experiments given that the concentration can only be increased to a certain degree to maintain true Brownian motion and limited power available to the laser. Therefore interaction studies with this nanomaterial and lipid vesicles were not possible.

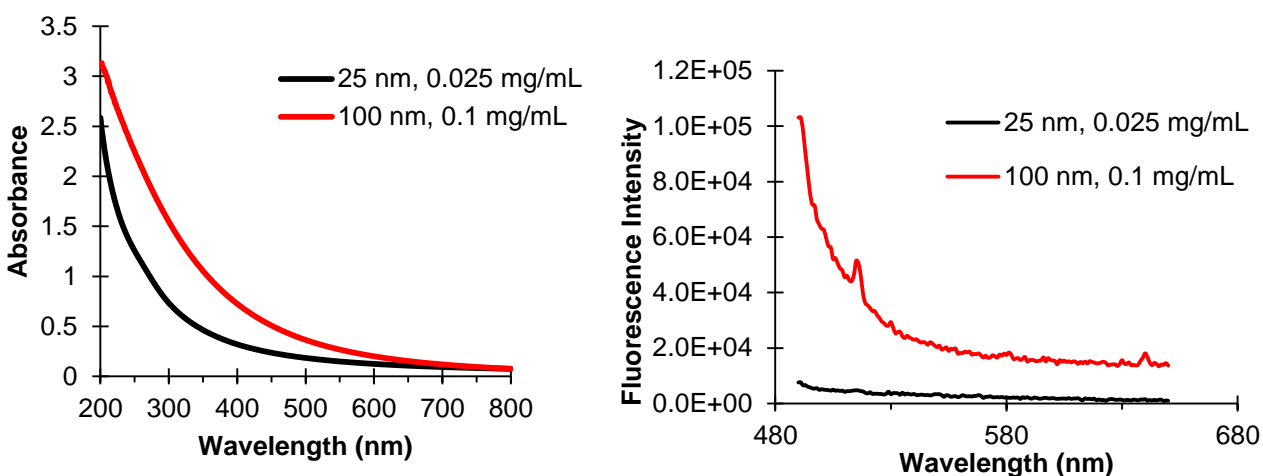


Figure 2.4. A) Uv-Vis absorbance spectra and B) fluorescence emission spectra at 470 nm excitation of the two Nv ND types.

2.3 References

1. Kapusta, P. Absolute Diffusion Coefficients: Compilation of Reference Data for FCS Calibration.
http://www.picoquant.com/images/uploads/page/files/7353/appnote_diffusioncoefficients.pdf (accessed September 23).
2. Troiano, J. M.; Olenick, L. L.; Kuech, T. R.; Melby, E. S.; Hu, D.; Lohse, S. E.; Mensch, A. C.; Dogangun, M.; Vartanian, A. M.; Torelli, M. D.; Ehimiaghe, E.; Walter, S. R.; Fu, L.; Anderton, C. R.; Zhu, Z.; Wang, H.; Orr, G.; Murphy, C. J.; Hamers, R. J.; Pedersen, J. A.; Geiger, F. M., Direct Probes of 4 nm Diameter Gold Nanoparticles Interacting with Supported Lipid Bilayers. *The Journal of Physical Chemistry C* **2015**, 119 (1), 534-546.
3. van Meer, G.; Voelker, D. R.; Feigenson, G. W., Membrane lipids: where they are and how they behave. *Nat Rev Mol Cell Biol* **2008**, 9 (2), 112-124.
4. Yang, J. A.; Murphy, C. J., Evidence for Patchy Lipid Layers on Gold Nanoparticle Surfaces. *Langmuir* **2012**, 28 (12), 5404-5416.

Chapter 3: CONCLUSIONS AND FUTURE WORK

Important steps were made in understanding possible lipid corona formation on fluorescent polystyrene nanoparticles through fluorescence correlation spectroscopy. It was shown that the hydrodynamic diameter of PS/NH₂ nanoparticles increased upon incubation with lipid vesicles and suggesting bilayer formation or multiple bilayer formation. The poor fluorescence of Nv ND hindered its use in lipid vesicle experiments, in particular because these experiments are done *in situ*.

The following PEG-terminated polystyrene nanoparticles (5000 MW) will be prepared via the EDC coupling mechanism to provide a neutral nanoparticle for these studies and to determine the mechanism of lipid corona formation. Systematic variation of the lipid vesicle fluidity can help explain the effect fluidity to lipid corona formation. Addition of lipid vesicle may result in slight changes of sample viscosity that can confound the data, therefore viscosity checks should be done to each sample to determine if the samples change viscosity.

Cryo-TEM imaging of nanoparticle following addition of lipid vesicle should hopefully allow us to visualize lipid around the polystyrene nanoparticles, in its near native state. These studies need to be repeated for robust results of lipid corona formation. Further studies would include XPS or MS studies for quantification of lipids on the polystyrene nanoparticles. Isothermal titration calorimetry can be used to obtain thermodynamic values of lipid adsorption onto polystyrene nanoparticles.